## RESEARCH ARTICLE

**Key Points:**
- CO$_2$ efflux data show no pattern with latitude
- Flow intensity is a primary control on CO$_2$ efflux and $p$CO$_2$ a secondary control
- Water surface appearance has potential as a proxy for flow intensity aiding rapid upscaling

# Hydraulics are a first-order control on CO$_2$ efflux from fluvial systems

Hazel Long[1], Leena Vihermaa[1], Susan Waldron[1], Trevor Hoey[1], Simon Quemin[1,2,3,4], and Jason Newton[5]

[1]School of Geographical and Earth Sciences, University of Glasgow, Glasgow, UK, [2]ENSTA ParisTech, Palaiseau, France, [3]Now at Centre of Geopolitics of Energy and Raw Materials, Paris-Dauphine University, Paris, France, [4]Now at Climate Economics Chair, Paris, France, [5]Scottish Universities Environmental Research Centre, East Kilbride, UK

**Abstract** Evasion of carbon dioxide (CO$_2$) from fluvial systems is now recognized as a significant component of the global carbon cycle. However, the magnitude of, and controls on, this flux remains uncertain, and improved understanding of both is required to refine global estimates of fluvial CO$_2$ efflux. CO$_2$ efflux data show no pattern with latitude suggesting that catchment biological productivity is not a primary control and that an alternative explanation for intersite variability is required. It has been suggested that increased flow velocity and turbulence enhance CO$_2$ efflux, but this is not confirmed. Here using contemporaneous measurements of efflux (range: 0.07–107 $\mu$mol CO$_2$ m$^{-2}$ s$^{-1}$), flow hydraulics (mean velocity range: 0.03–1.39 m s$^{-1}$), and $p$CO$_2$ (range: 174–10712 $\mu$atm) at six sites, we find that flow intensity is a primary control on efflux across two climatically different locations (where pH is not a limiting factor) and that the relationship is refined by incorporating the partial pressure of CO$_2$ ($p$CO$_2$) of the water. A remaining challenge is how to upscale from point to reach or river basin level. Remote imaging or river surface may be worth exploring if subjectivity in interpreting surface state can be overcome.

## 1. Introduction

Fluvial systems are often oversaturated with carbon dioxide (CO$_2$) and thus have the capacity to degas CO$_2$ to the atmosphere [*Butman and Raymond*, 2011; *Melack*, 2011; *Billett et al.*, 2006]. Such evasion of CO$_2$ is now recognized to be a significant component of the global carbon cycle, estimated at a rate of $1.8 \pm 0.25$ Pg of carbon per year [*Raymond et al.*, 2013], and its omission from carbon budget calculations may account for some of the imbalance in global estimates of carbon reservoir size and rate of transfer [*Richey et al.*, 2002; *Billett et al.*, 2006; *Aufdenkampe et al.*, 2011]. While efflux estimates are becoming more precise, and a significant amount of carbon is known to be reprocessed within fluvial systems in a series of transformations and losses [*Cole et al.*, 2007; *Tranvik et al.*, 2009], the specific controls on CO$_2$ efflux and its exact magnitude remain poorly understood and quantified [*Zappa et al.*, 2007; *Alin et al.*, 2011; *Butman and Raymond*, 2011; *Rasera et al.*, 2013] and fluvial CO$_2$ evasion may still be underestimated [*Alin et al.*, 2011; *Raymond et al.*, 2013] or overestimated [*Hunt et al.*, 2011; *Abril et al.*, 2015]. As such we need to better quantify and understand the controls on aquatic CO$_2$ degassing, particularly in systems, such as rivers and lower order streams, for which data remain sparse [*Butman and Raymond*, 2011; *Melack*, 2011; *Wallin et al.*, 2011].

Published CO$_2$ efflux data show similar means and ranges from rivers across a wide latitudinal range (Figure 1 and supporting information Figure S1). This contradicts expectation of intersite variability in CO$_2$ efflux in response to drivers of the fluvial CO$_{2(aq)}$ pool size, for example, soil type, geology, temperature, and river water pH (Table 1) [*Rebsdorf et al.*, 1991; *Aufdenkampe et al.*, 2011; *Lauerwald et al.*, 2013]. Further, where moisture is not a limiting factor, catchment biological productivity is greater in warmer environments [*Lauerwald et al.*, 2013; *Maberly et al.*, 2013], and greater productivity in a catchment has been linked to increased riverine CO$_2$ concentrations and CO$_2$ efflux [*Maberly et al.*, 2013]. Thus, in the tropics and equatorial regions CO$_2$ efflux from fluvial systems may be expected to be greater than at higher latitudes. However, no consistent increase in CO$_2$ efflux rate with decreasing latitude is observed (Figure 1), suggesting that net ecosystem productivity [e.g., *Crammer et al.*, 1999] is not a primary control on CO$_2$ efflux.

Studies of the controls on oxygen aeration [e.g., *Moog and Jirka*, 1998; *Palumbo and Brown*, 2013] have shown how a range of hydraulic factors, including velocity, depth, and channel slope, can be used to produce statistical equations, which can be used to calculate the capacity for fluvial systems to absorb gas from the
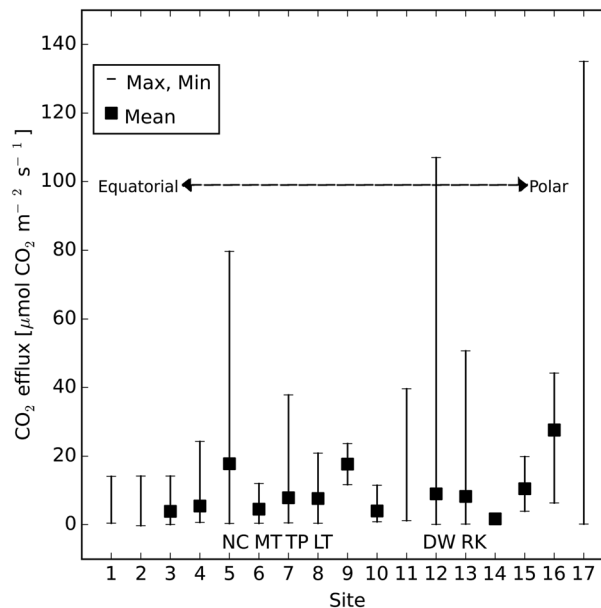
**Figure 1.** Global $CO_2$ flux rates, obtained by direct measurement from flowing water, displaying maximum, minimum, and mean $CO_2$ efflux values. Data sources and site references are in Table 1. Sites are ordered by latitude. Site locations shown in Figure S1.

atmosphere. While these studies provide understanding of gas fluxes, there is a range of forms of the predictive relationships and recognition that existing approaches are restricted by the range of flow depths and velocities for which gas transfer data are available and by the quality of the overall database [*Palumbo and Brown*, 2013]. In essence, gas transfer across the air-water interface occurs by molecular diffusion [*Moog and Jirka*, 1999], at a rate controlled by the concentration gradient. The rate of diffusion is also controlled by the thickness of the surface concentration boundary layer, i.e., the mean distance over which the gas concentration varies from the surface to nearly the bulk value [*Moog and Jirka*, 1999], and so thicker boundary layers reduce the rate of diffusion. Processes that disrupt the boundary layer therefore facilitate faster diffusion and so greater gas efflux [*Jonsson et al.*, 2008]. In the ocean and lakes, wind drag on the water surface creates surface waves [*Liss and Merlivat*, 1986; *Wanninkhof*, 1992; *Bock et al.*, 1999; *Hofmann et al.*, 2008] and so enhances diffusion and increases gas fluxes. Wind plays the same roles in rivers as in the ocean and lakes, but this effect is spatially and temporally restricted. In estuaries and large rivers, wind can be the dominant physical control on gas exchange, but upstream in smaller channels, such as mainly measured here, stream characteristics which control the hydraulic properties of the flow are more significant [*Alin et al.*, 2011]. The interaction of downslope flow of water and channel roughness generates turbulence within the water column and energy dissipation in the form of surface waves when the flow reaches a critical state [*Gordon et al.*, 2004] disrupting the surface boundary layer. It has been observed that high turbulent energy during high river flow enhances fluvial gas evasion [*Hope et al.*, 2001; *Billett et al.*, 2006; *Billett and Moore*, 2008; *Butman and Raymond*, 2011; *Wallin et al.*, 2011; *Raymond et al.*, 2013; *Rasera et al.*, 2013], but the nature of this effect has not been confirmed by direct, contemporaneous measurements of flow state and $CO_2$ efflux.

Given the strong rationale for how hydraulic characteristics may influence the rates of riverine $CO_2$ effluxes, and the homogeneity observed in measured $CO_2$ efflux globally (Figure 1), we designed a research program to assess the importance of flow hydraulics on $CO_2$ efflux. As climate change is projected to change regional hydrology, including seasonality, [e.g., *Gloor et al.*, 2013; *Charlton and Arnell*, 2014] understanding whether flow characteristics exert a physical control on efflux rate is required to measure the impact of climate change on $CO_2$ feedback processes.

Here at sites in two distinct climatic and hydrological regions, we assess whether flow intensity (a generic term which describes one or more of the measures of flow strength including mean flow velocity, bed shear stress, turbulent stress, and flow state) is a primary control on $CO_2$ efflux through simultaneous field measurements of $CO_2$ efflux, flow hydraulics, and other environmental descriptors. We explore an approach for supporting upscaling from point to provide catchment scale (or larger) flux estimates.

## 2. Materials and Methods

Our field sites vary in location, size, and catchment characteristics, and sampling has been carried out over several years, thus capturing a range of seasons and flow conditions. Within each site, measurement locations were chosen to ensure that a range of flow intensities were included.

**Table 1.** Global $CO_2$ Efflux Rates From Flowing Water[a]

| Site Code | Site | Location | Catchment | Time Period | Method | Min.; Max. Efflux | Mean; Median Efflux | Mean (Min.; Max.) $pCO_2$ | Source |
|---|---|---|---|---|---|---|---|---|---|
| DW | Drumtee Water | Scotland | Agriculture/peat | 6/12 to 12/13 | FC | 0.07; 107 | 9.00; 2.59 | 1136 (174; 2678) | This study |
| RK | River Kelvin | Scotland | Urban | 6/12 to 12/13 | FC | 0.16; 50.7 | 8.25; 4.68 | 1112 (301; 1956) | This study |
| MT | Main Trail | Amazon | Rainforest | 2/11 to 5/12 | FC | 0.40; 12.0 | 4.54; 4.61 | 2451 (1256; 4205) | This study |
| NC | New Colpita | Amazon | Rainforest | 2/11 to 5/12 | FC | 0.33; 79.7 | 17.8; 13.2 | 6163 (2399; 10712) | This study |
| LT | La Torre | Amazon | Rainforest | 2/11 to 5/12 | FC | 0.40; 20.9 | 7.64; 6.65 | 2277 (742; 4397) | This study |
| TP | Tambopata | Amazon | Rainforest/Agriculture/mining | 2/11 to 5/12 | FC | 0.50; 37.8 | 7.87; 6.48 | 1577 (813; 2965) | This study |
| 1 | Amazon Basin | Brazil | Agroecosystems | 7/06 to 5/07 | FC | 0.41; 14.1[z] | - | - | Rasera et al. [2008] |
| 2 | Amazon Basin | Various | Various | 1/06 to 12/10 | FC, CP | −0.2; 14.2[z] | - | −(259; 7808)[x] | Rasera et al. [2013] |
| 3 | Amazon | Various | Various | 6/04 to 1/07 | FC | 0.04; 14.2 | 3.90; — | 3317 (619; 12616) | Alin et al. [2011] Large Rivers[x] |
| 4 | Mekong basins | Various | Various | 6/04 to 1/07 | FC | 0.67; 24.3 | 5.45; — | 3353 (141; 9569) | Small Rivers[y] |
| 9 | Amazon Basin | Brazil | Gneiss bedrock Oxisol soil | 1/07 to 1/08 | FC | 11.7; 23.7[z] | 17.7; — | −(6491; 14976) | Neu et al. [2011] |
| 10 | Mer Bleue Peatland | Canada | Peatland | 4/05 | FC | 0.82; 11.5 | 3.99; — | - | Billett and Moore [2008] Flowing water |
| | Mer Bleue Peatland | Canada | Peatland | 4/05 | FC | 0.20; 1.84 | 0.80; — | - | Open water |
| | Mer Bleue Peatland | Canada | Peatland | 4/05 | FC | 0.20; 11.5 | 2.39; — | −(3850; 8630) | All data |
| 11 | Black Burn | Scotland | Peatland | 1/05-8/05 | FC | 1.17; 39.6 | - | - | Billett et al. [2006] |
| 14 | Brocky Burn | Scotland | Mixed[b] | 3/97 to 8/98 | CC, GT | 0.25; 3.20 | 1.70; — | 424 (—; —) | Hope et al. [2001] Lower reaches |
| 15 | Brocky Burn | Scotland | Mixed | 3/97 to 8/98 | CC, GT | 3.91; 19.9 | 10.5; — | 1361 (—; —) | Middle reaches |
| 16 | Brocky Burn | Scotland | Mixed | 3/97 to 8/98 | CC, GT | 6.33; 44.2 | 27.6; — | 2674 (—; —) | Upper reaches |
| 17 | Krycklan Catchment | Sweden | Podzol soil and glaciofluvial sediment | 06 to 07 | FC | 0.16; 135 | - | −(713; 6253) | Wallin et al. [2011] |

[a]Efflux in $\mu mol\ CO_2\ m^{-2}\ s^{-1}$, $pCO_2$ in $\mu atm$. Site codes correspond to Figure 1 and locations displayed in Figure S1. Method codes; FC = floating chamber, CP = water/atm $pCO_2$ difference and gas transfer velocity, CC = $CO_2$ concentration of the water, GT = gas tracer. [x]Rivers > 100 m wide. [y]Rivers < 100 m wide. [z]Min. and max. efflux calculated using standard deviations.
[b]Mixed: Granite bedrock, glacial drift, and organic soils.

## 2.1. Field Study Sites

Measurements were made in two catchments in the UK and one in the Peruvian Amazon. The UK measurements were made in two rivers with different land uses and catchment sizes, the River Kelvin (RK) and Drumtee Water (DW). The Kelvin (sampling site 55°52′06″N, 4°17′16″W; 18 m above sea level (asl)) is a 335 km$^2$ semiurban (23%) catchment, containing agricultural land (70%) and some forestry (6%), with a maximum elevation within the catchment of 510 m. Measurements were made within a 30 m reach, 1.2 km upstream of the confluence with the River Clyde Estuary, where bankfull width is 15–20 m and bed sediment is large pebbles and patches of exposed bedrock. Drumtee Water (sampling site 55°41′16″N, 4°23′37″W; 197 m asl) is a headwater, 9.6 km$^2$, peat-dominated catchment where the land use is rough grazing and maximum elevation within the catchment is 260 m. Measurements were made in a 19 m reach, where the channel is 4–5 m wide. These two drainage systems were sampled between June 2012 and December 2013 (number of samples: RK 83 and DW 79).

In the Amazon, measurements were made in four fluvial systems draining tropical rainforest in the Tambopata National Reserve (12°50′00″N, 69°17′45″W; 200 m asl), Madre de Dios region, Peru (for site map see *Vihermaa et al.* [2014]). The sites ranged from small streams draining the local forest area to large rivers. Main Trail (MT) has a catchment of ~5 km$^2$ and was only active during the rainy season, being fed by surface runoff and throughflow. New Colpita (NC) is a perennial small stream draining 7 km$^2$. In both cases, channels were 4–7 m wide at sampling locations, width varying with season and corresponding stage height. La Torre river (LT) drains an area of 2000 km$^2$, and the channel is 40–80 m wide at the sampling point, which is located close to the confluence with Tambopata river (TP). TP has a 14,000 km$^2$ catchment extending to the foothills of the Andes, and the channel at the sampling point was ~200 m wide. TP catchment contains some small-scale agriculture and gold mining, but all four catchments are predominantly rainforest. The Amazonian sites were sampled between February 2011 and May 2012 with sampling campaigns including both wet and dry seasons and targeting the associated different water levels and flow conditions (number of samples: MT 42, NC 46, LT 37, and TP 26).

## 2.2. CO$_2$ Efflux

In all cases CO$_2$ efflux was quantified from measuring the rate of CO$_2$ accumulation in a floating chamber of known volume (0.0029 m$^3$) [*Frankignoulle*, 1988] using a Licor (LI-840A) infrared CO$_2$/H$_2$O gas analyzer (for configuration see supporting information Figure S2). CO$_2$ accumulation was measured over 4 min and repeated three times. CO$_2$ flux was calculated using equation (1) [*Frankignoulle*, 1988; *Rasera et al.*, 2008]:

$$F_{CO2} = \left(\frac{\delta CO_2}{\delta t}\right)\left(\frac{V}{RTS}\right) \tag{1}$$

where $F_{CO2}$ is the flux ($\mu$mol CO$_2$ m$^{-2}$ s$^{-1}$), $\delta CO_2/\delta t$ is the slope of CO$_2$ accumulation in the chamber ($\mu$atm s$^{-1}$), $V$ is the chamber volume (m$^3$), $R$ is the gas constant (m$^3$ atm K$^{-1}$ mol$^{-1}$), $T$ is the air temperature (K), and $S$ is the surface area of the chamber at the water surface (m$^2$).

## 2.3. Hydraulic Parameters

In the UK rivers, velocity was measured using a Valeport flowmeter with 50 mm diameter impeller, set to 60 second averaging, at 20% and 80% of the flow depth (for depth-averaged mean calculations) and a minimum of three other heights (to allow identification of outliers) within the semilogarithmic lower part of the flow profile. Mean velocity ($\bar{u}$ m s$^{-1}$) is an indicator of depth-averaged hydraulic conditions at the measurement point. Flow characteristics can be explored by considering the Froude (*Fr*) and Reynolds (*Re*) numbers. *Fr* is a depth-averaged dimensionless number that indicates the amount of surface water disturbance such as waves [*Gordon et al.*, 2004; *Allen*, 1997] and so can act as a proxy for the interaction and degree of gas exchange between the water surface and the atmosphere. Reynolds number (*Re*) indicates the degree of turbulence and hence mixing in the water column [*Gordon et al.*, 2004] and is an indicator of the potential transfer of CO$_2$-enriched water from lower in the water column and hyporheic zone (e.g., benthic recharge) [*Peter et al.*, 2014] to the water surface. Froude and Reynolds numbers are calculated as follows:

$$a) \quad Fr = \frac{\bar{u}}{\sqrt{gH}} \tag{2a}$$

$$b) \quad Re = \frac{\bar{u}H}{v} \tag{2b}$$

where $g$ is the acceleration due to gravity ($m\,s^{-2}$), $H$ is the water depth (m), and $\nu$ is the kinematic viscosity ($m^{-2}\,s^{-1}$). Additionally at the UK sites, a qualitative visual assessment of the water surface state was undertaken; i.e., the degree of surface disturbances was estimated at the time of the $CO_2$ efflux measurement: "smooth" (a flat water surface), "medium" (ripples/waves with no white water) or "rough" (ripples and waves with white water) (for examples of these states see supporting information Figure S9). Wind speed was not measured, although the visual classification of water surface state incorporates the effect of wind at the water surface.

In the Amazonian streams, near-surface flow velocity is the mean of three replicates taken directly below the chamber position using a Geopacks hand-held flowmeter. Information to calculate $Re$ and $Fr$ was not available from the Amazon sites. As $\bar{u}$ is highly correlated with $Fr$ and $Re$, by definition, $\bar{u}$ is used alone to indicate flow intensity for the Amazonian sites.

## 2.4. Water Chemistry Parameters

Water chemistry was analyzed at the time of chamber deployment to allow calculation of $p$CO$_2$ and exploration to find explanatory variables for $CO_2$ flux models. At Drumtee Water, pH was logged continuously (at 30 min resolution) with an In-Situ Inc. MP TROLL 9000 water chemistry sonde. The Troll 9000 was calibrated approximately every 4 to 6 weeks using two point calibrations from freshly prepared pH 4 and pH7 buffer solutions, and ensuring the manufacturers specified acceptable values for slope and intercept were reached. Measuring pH in situ eliminated the possibility of a delay enabling microbial action that leads to an altered sample pH [*Abril et al.*, 2015] and avoided compromising sample integrity through laboratory processes (which can alter sample pH through artificial degassing) [*Herczeg and Hesslein*, 1984; *Abril et al.*, 2015]; measuring pH continuously met the manufacturers pH probe minimum equilibration time specification of 20 min. For the River Kelvin our directly measured pH data were unreliable due to equipment malfunction and so pH was calculated from a linear relationship ($n = 10$; $R^2 = 0.72$) between discharge and pH fitted to data collected at a monitoring station 9 km upstream of the $CO_2$ measuring site (data provided by the Scottish Environmental Protection Agency, 2015). There are no significant tributaries entering between these sampling points, and similarity in water chemistry has been verified in a separate spatial sampling experiment (for details see supporting information Figure S3). At both RK and DW air and water temperature were measured using a Lilipop®, Traceable®, handheld thermometer.

For MT and NC, pH, conductivity and temperature were logged at 15 min resolution by an In-Situ Inc. MP TROLL 9500 data logger. For LT and TP, spot measurements of pH, conductivity, and temperature were made using a TROLL 9500 data logger at the time of $CO_2$ flux measurement. The TROLL was deployed for >20 min to ensure equilibration with stream water, and a maintenance regime similar to that described earlier was used.

At all sites, within 15 min of the flux measurement, water samples were collected for determining dissolved inorganic carbon concentration ([DIC]) using a headspace method [*Waldron et al.*, 2014] and analysis on a Thermo-Fisher-Scientific Gas Bench/Delta V Plus. Partial pressure of $CO_2$ ($p$CO$_2$) was calculated from the [DIC] using pH and temperature [*Rebsdorf et al.*, 1991; *Stumm and Morgan*, 1996]. Where pH was measured using a Troll 9000 or 9500 (DW, NC, MT, LT, and TP), uncertainty in pH is ±0.1 pH unit according to the manufacturers specifications and 1.3% for RK indicated by the percent residuals (Figure S3). Uncertainty in [DIC] is 0.027 nM [*Waldron et al.*, 2014].

## 2.5. Data Analysis

Data analysis was carried out using R statistical package version 3.1.0 [*R Development Core Team*, 2008]. Most of the measured variables were lognormally distributed (Figure 3) and were log-transformed prior to modeling. As multiple measurements were made at each site, the data show some clustering. Thus, to avoid pseudoreplication in the analysis, a linear mixed effect model was fitted to the data [*Pinheiro et al.*, 2014]. Initially, a null model with no explanatory variables was fitted to the data to investigate the influence of different levels of data structure. This showed that 2% of the variance was between regions (Amazon; UK), 12% between sites within a region, and 86% within the sites. The low between site and between region variances suggest that there was no significant systematic regional difference in efflux rate. The 86% of variance within the individual sites indicates that the differences in site characteristics (e.g., stream order) were less important than sample-to-sample variability due to variation in flow intensity and water chemistry. Further,
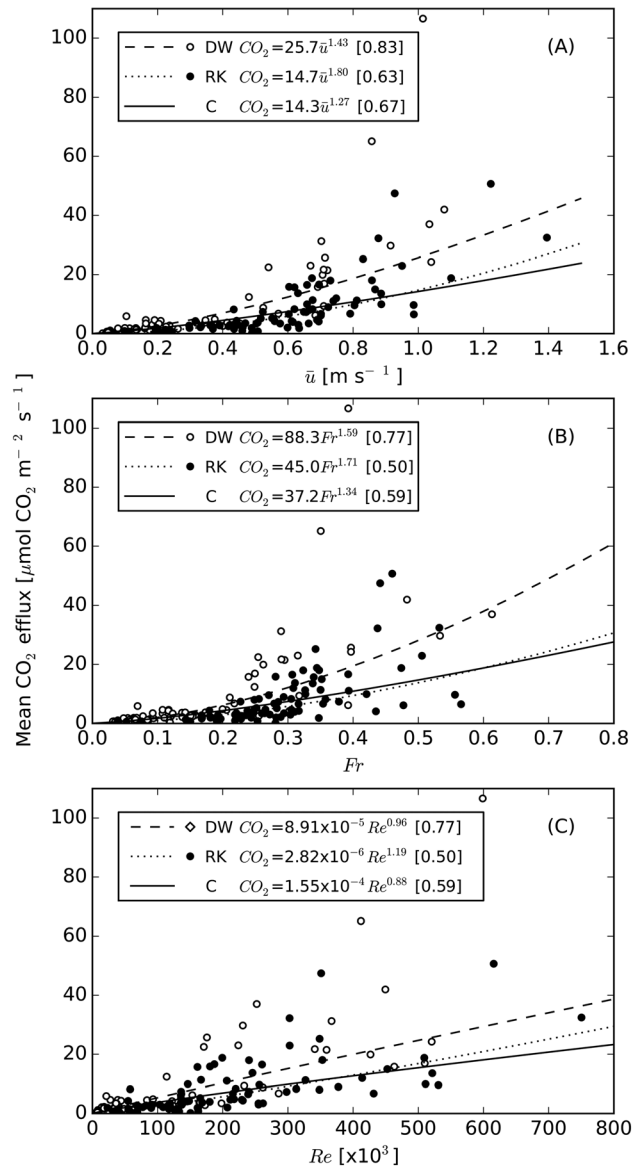
**Figure 2.** $CO_2$ fluxes related to hydraulic properties for DW and RK sites. $CO_2$ efflux plotted against: (a) mean flow velocity ($\bar{u}$), (b) Froude number ($Fr$), and (c) Reynolds number ($Re$). All show strong positive, logarithmic relationships with $CO_2$ efflux, with efflux rates being slightly higher and the curves slightly steeper at DW. "C" represents DW and RK combined data. All relationships were significant at $P < 0.001$. $R^2$ values (in square brackets) indicate that the relationship between $\bar{u}$ and $CO_2$ efflux is strongest.

analysis of the variance structure indicated that "site" was sufficient as a grouping factor in further analyses as regional variance was so low.

## 3. Results

$CO_2$ efflux rates ranged between 0.07 and 107 $\mu mol\,CO_2\,m^{-2}\,s^{-1}$ overall, with all six sites having similar $CO_2$ efflux ranges. Five sites had very similar mean $CO_2$ effluxes (range 4.54 to 9.00 $\mu mol\,CO_2\,m^{-2}\,s^{-1}$); however, the mean at NC was 17.8 $\mu mol\,CO_2\,m^{-2}\,s^{-1}$, two to four times that of the other sites. Ranges and means of $CO_2$ efflux rates at all sites lie within the range of previously reported values (Figure 1 and Table 1).

Using pooled data from DW and RK, significant positive logarithmic correlations are found between $CO_2$ efflux and each of the hydraulic parameters, $\bar{u}$, $Fr$, and $Re$ (Figure 2). Data from RK and DW overlap indicating similar controls on efflux at both sites, although with some differences in the gradients and significance levels of the relationships (Figure 2). At all six sites there was a significant positive correlation between $CO_2$ efflux and $\bar{u}$ (Figure 3), although the overall relationship shows fanning at the upper end. The similarity of relationships involving $\bar{u}$, $Fr$, and $Re$ with efflux occurs by definition, but turbulence and flow state are responsible for gas transfer within the water column and at the water-atmosphere boundary, respectively. Mean velocity empirically records these processes but is less likely to be applicable across scales than the dimensionless $Fr$ and $Re$ parameters. However, $\bar{u}$ has the highest correlation with $CO_2$ efflux at the UK sites and is the only measure of

flow intensity available for the Amazon data, so we use mean velocity below acknowledging that this is an empirical proxy for turbulence and water surface conditions. For generality, we use the term flow intensity to encompass the combined effects of velocity, turbulence, and water surface conditions on gas transfer and exchange.

$CO_2$ partial pressure of the water ($pCO_2$) varied between sites, and all were within previously reported ranges [*Raymond et al.*, 2013, and references therein] (Table 1). NC had by far the highest $pCO_2$ of all the studied sites (mean 6163 $\mu atm$, maximum 10,712 $\mu atm$) with mean $pCO_2$ being 2.5–5.5 times the magnitude of that of the other sites. RK had the lowest mean and maximum $pCO_2$ (mean 1112 $\mu atm$, maximum 1956 $\mu atm$) with the maximum $pCO_2$ being lower than the minimum $pCO_2$ at NC (2399 $\mu atm$). We propagated the pH and DIC
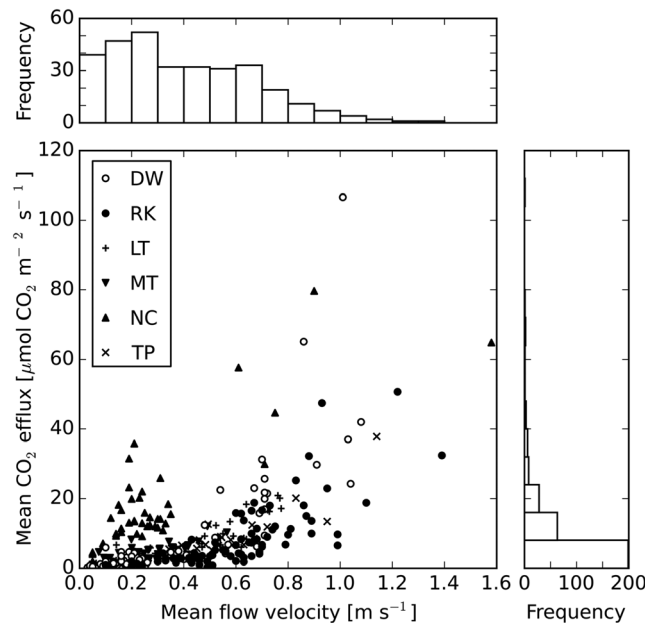
**Figure 3.** $CO_2$ efflux and mean flow velocity data from all UK and Amazonian sites. All sites follow the same trend whereby $CO_2$ efflux increases with flow velocity, apart from one of the Amazonian small streams (NC) where a given velocity resulted in a higher efflux rate. Both the response variable (efflux) and the explanatory variable (flow velocity) show skewed distributions and were therefore log-transformed before fitting statistical models to the data.

uncertainties to calculate the uncertainty in $pCO_2$; this ranges from 14.4 to 32.8% of the $pCO_2$ value, and the intersite differences still exist; for example, NC is significantly different to the other sites ($P = <0.001$; for detail see supporting information Table S1 and Figure S4).

The relationship between $CO_2$ efflux and $\bar{u}$ at the Amazonian sites was the same as the UK sites (Figure 3), except for at NC which has a higher rate of $CO_2$ efflux for a given velocity. When the influence of $pCO_2$ was included, by plotting efflux against the product of flow velocity and $pCO_2$, data from NC and all other sites collapse onto a linear log-log relationship (Figure 4). Assumptions that all error is contained in either the product of flow velocity and $pCO_2$, or flux provide constraints on the range in this relationship (Figure 4).

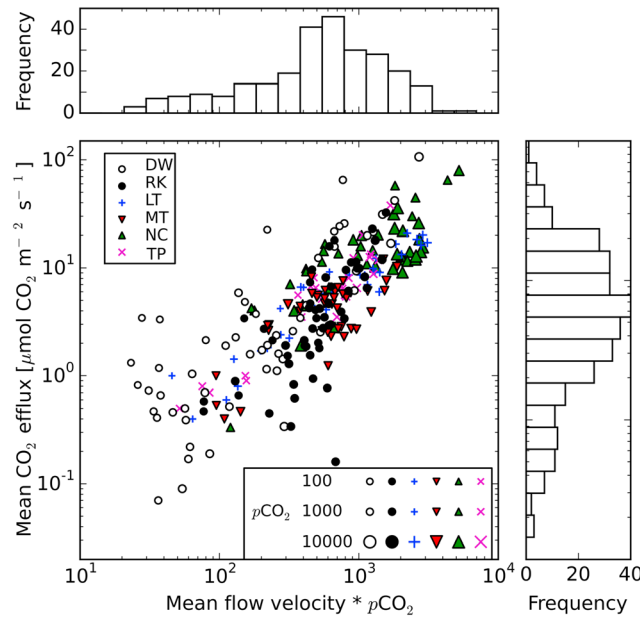A multiple regression model, with log-transformed flow velocity and $pCO_2$ as explanatory variables, describes the data from all six sites (equation (3)). The residuals were randomly distributed (see supporting information Figure S5):

$$\log(F_{CO2}) = -2.88 + 1.06 * \log(\bar{u}) + 0.77 * \log(pCO_2). \qquad (3)$$

The fit had an adjusted $R^2$ value of 0.66 (see supporting information Figure S6), and the overall $P$ value was highly significant ($<0.001$). An alternative approach fitting a model with flow: $pCO_2$ interaction was also tested, but the interaction term was not significant.

To account for intersite variation, a linear mixed effect model was fitted [*Pinheiro and Bates*, 2000], which yielded the following predictive equation based on the fixed effects:

$$\log(F_{CO2}) = 1.43 + 1.20 * \log(\bar{u}) + 0.22 * \log(pCO_2). \qquad (4)$$

Site-specific random effect terms on the intercept ranged from $-0.87$ to $+1.12$ (see Figure S6). In this case the flow:$pCO_2$ interaction term was autocorrelated with $pCO_2$ and could not be included in the model simultaneously. The site-specific terms reflect the magnitude of $CO_2$ efflux and thus are related to site-specific controls over the availability of $CO_2$. Four sites have effect terms that are close to zero ($-0.14$ to 0.01); RK has a significantly lower intercept ($-0.87$) and NC a significantly higher value (1.12).

The two models, equations (3) and (4), have different intercepts due to the separate site-specific component in the mixed effects model. The flow velocity coefficients (1.06 and 1.20) are similar between the models but $pCO_2$ has a lower coefficient in the mixed effects model (0.77 versus 0.22). This implies that some of the differences in $pCO_2$ values between sites (Kruskal-Wallis rank sum test, $P$ value $\ll 0.001$) are attributed to site-specific effects, whereas the velocity differences are systematic across all sites.

Direct measurement of hydraulic properties is not always possible, so for the UK sites, the qualitative description of water surface state was used to assess the potential for rapid upscaling. Adding water surface state to the logarithmic relationships between efflux and hydraulic variables, the data separate according to the visual characterization (Figure 5). There is little separation between the medium and rough data sets, implying that moderate disturbance of the water surface disrupts the surface boundary layer.

**Figure 4.** Data from UK (RK and DW) and Amazonian sites (MT, NC, LT, and TP) demonstrating a log-log relationship between $CO_2$ efflux and the product of flow velocity and $pCO_2$. By including the influence of $pCO_2$, NC falls in line with the rest of the study sites. The log-transformation produces variables that are approximately normally distributed as shown by the histograms. Symbol size is scaled by $pCO_2$, and site coded by color. The dashed and dotted lines are log-log regressions assuming that all error is contained in flux and the "mean flow velocity*$pCO_2$" product, respectively. The solid line is the bisector of these relationships and is an approximation to the functional relationship between the dependent and independent variables where both have equal proportional error.

## 4. Discussion

Measurements of the ranges and mean values of $CO_2$ efflux from rivers in contrasting climatic zones, UK (temperate) and Amazonian (tropical), show no significant differences, and all data fall within previously reported ranges that show no consistent pattern with latitude (Figure 1 and Table 1). We interpret these results as showing that ecosystem level productivity is not the primary control on $CO_2$ efflux and an alternative explanation for intersite variability in $CO_2$ efflux is required.

pH can limit $CO_2$ efflux through its influence on speciation of the DIC pool [*Hoffmann and Schellnhuber*, 2010]. At high pH, a greater proportion of the DIC pool is in the form of carbonate and bicarbonate ions, which only exist in aqueous form, and so are not available for degassing. Thus, it is possible that at higher pH the $CO_2$ pool size may be smaller; however, the size of the $CO_2$ pool is also dependent on the total DIC concentration, as it is a proportion of this. Here at the time of sampling,

the pH of all fluvial systems was rarely above pH 7; thus, in all cases, under these relatively low pH conditions, $CO_2$ was available for degassing.
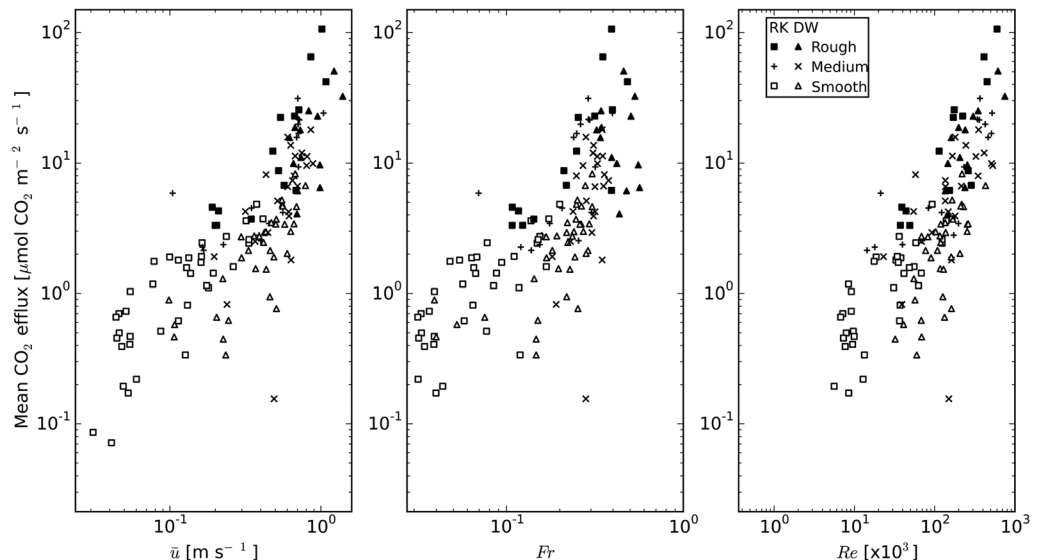


**Figure 5.** Separation of data by visually determined flow state in the relationships between $CO_2$ efflux and mean velocity, Froude number, and Reynolds number.

Within-site variability is greater than that observed between sites and is consistently related to flow hydraulics (Figures 3 and 4). Hydraulic controls over $CO_2$ efflux have been suggested previously [*Raymond et al.*, 2012; *Wallin et al.*, 2011], but published studies estimated this from stream slope and estimates of gas transfer velocity ($k$) rather than direct measurements of both flux and hydraulic variables as have been made here. When pooled $CO_2$ efflux data from all six sampling sites were plotted against $\bar{u}$, an increase in $CO_2$ efflux occurs as flow intensity increases regardless of climatic zone (Figure 3). $CO_2$ efflux should be enhanced by flow intensity because convection and turbulent mixing associated with eddies greatly enhance gas transfer across the air-water interface [*Moog and Jirka*, 1999; *Eugster et al.*, 2003] by repeatedly renewing the surface boundary layer with $CO_{2(aq)}$, maintaining a steep $CO_2$ concentration gradient between the water and the atmosphere [*Eugster et al.*, 2003]. It is unclear what scale of eddies are the most important to gas transfer across an air-water interface [*Moog and Jirka*, 1999]. However, it is thought to be a combination of large- and small-scale eddies, with the higher-frequency small-scale eddies embedded within larger eddies, carried to the surface where they renew the surface zone [*Moog and Jirka*, 1999], transferring $CO_2$ where available from the bed.

Of all of the sites, NC is distinctive having higher minimum, maximum and mean $CO_2$ efflux than the other five sites for a given flow velocity (Figure 3 and Table 1). At all six sites, mean $p$$CO_2$ levels showed oversaturation with respect to atmospheric $CO_2$ concentration, but NC had much higher $p$$CO_2$ levels and greater oversaturation than all the other sites (Table 1). Although data are not abundant, elevated $p$$CO_2$ has been previously reported to enhance $CO_2$ evasion [*Billett and Moore*, 2008]. Elevated $p$$CO_2$ can cause enhanced $CO_2$ efflux due to a greater availability of $CO_2$ for degassing and a steeper water-atmosphere $CO_2$ concentration gradient [*Billett et al.*, 2006]. Thus, it seems likely that at NC, the higher concentration of $CO_2$ in the water resulted in greater $CO_2$ efflux at a given velocity. When $p$$CO_2$ was included in the model for efflux, NC data aligned with the other sites (Figure 4 and supporting information Figure S7). That it was only necessary to include $p$$CO_2$ to align one site suggests flow intensity is the primary control on $CO_2$ efflux and $p$$CO_2$ the secondary. Our knowledge of hydrological pathways in the catchments supports this analysis, as NC is the only site with a dominant groundwater contribution to its flow. Fanning at the upper end of the relationship between $CO_2$ efflux and $\bar{u}$ (Figure 3) indicates that factors that were not considered in this study may contribute to variation in $CO_2$ efflux, for example, the interaction of stream water with the river bed [e.g., *Peter et al.*, 2014]), dissolved organic carbon concentration (as a contributor through respiration or UV oxidation to $CO_2$ [*Cole et al.*, 2007]), or seasonality (controlling allochthonous inputs and as a proxy for temperature, autochthonous and secondary production [e.g., *Billett and Moore*, 2008; *Dawson et al.*, 2009]).

These data suggest that for the range of $p$$CO_2$ values at the six sites, $CO_2$ efflux can be considered to be hydraulically limited, analogous to transport-limited solute transport in rivers; i.e., the flux of $CO_2$ to the atmosphere is primarily determined by turbulence and water surface disturbance which, respectively, supply $CO_2$ to the water surface and facilitate its transfer to the atmosphere. Figure 2 shows significant single-site relationships between efflux and flow parameters, with $R^2$ values 0.5–0.83. Combining data from sites introduces variation in $p$$CO_2$ and potentially other processes such as wind disturbing the water surface which is of more significance in larger rivers. However, introducing $p$$CO_2$ either as a secondary variable (equation (3)) or in a linear mixed effect model (equation (4); Figure 4) provides improved statistical significance. Where the supply of $CO_2$ is limited, for example, in high pH streams, we hypothesize that the relative significance of hydraulic conditions will be reduced and that additional biogeochemical parameters may need to be introduced to these explanatory models.

As yet there is no simple sensor technology to directly measure $CO_2$ efflux from a stream or river surface and to enable spatial and temporal upscaling, so we need to explore proxy approaches. When considering the water surface state in the relationship between $CO_2$ efflux and log $\bar{u}$, log $Fr$ and log $Re$, the data separate according to the visual characterization of the water surface (Figure 5). The relationship between water surface state and Froude number is well known [*Gordon et al.*, 2004]: water surfaces classified as "smooth" separate by Froude number from those classified as medium and rough (supporting information Figure S8) and by definition, $Fr$ is correlated with other measures of flow intensity. With the collection of suitable calibration data sets, visual classification data could provide estimates of Froude number. Water surface state can be measured from aerial imagery [*Cox and Munk*, 1954; *Preisendorfer and Mobley*, 1986; *Gordon*, 2005] and so if this visual classification method can be refined, there may be potential for using remote sensing techniques to include more accurate estimates of $CO_2$ evasion from low-order and/or inaccessible streams in catchment scale or global estimates of riverine $CO_2$.

## 5. Conclusion

Direct measurements of flow intensity with $CO_2$ efflux rates at six sites in two contrasting climatic regions show that flow intensity is a primary control on $CO_2$ efflux rates. Here $\bar{u}$ has the highest correlation with $CO_2$ efflux but is less likely to be applicable across scales than $Fr$ and $Re$, so instead we use the term flow intensity to encompass multiple measures of flow stress. The relationship between flow intensity and $CO_2$ efflux is refined when $pCO_2$ is included in the model, correcting for intersite variability. The highest $CO_2$ effluxes were measured when both flow velocity and $pCO_2$ were high. However, the highest effluxes occur over a range of velocities, suggesting that additional controls, for example, diurnal or seasonal responses or the impact of hydrological events [e.g., *Peter et al.*, 2014] also influence $CO_2$ efflux rates. It may be possible to refine the model by quantifying these and incorporating such controls empirically into the model.

Having confirmed the significance of hydraulic controls over $CO_2$ efflux, there is potential for improving both the coverage and accuracy of $CO_2$ efflux estimates from surface waters, overcoming limitations in understanding that support upscaling. We note that our model describes less well $CO_2$ efflux rates at the highest flows and so further data are required in high flow conditions to refine the model. Additionally, we lack knowledge of $CO_2$ recharge from the interaction of the water column with the benthic and hyporheic zones [e.g., *Peter et al.*, 2014], and how this influences the capacity to degas $CO_2$ needs to be considered, with a view to comparison with models that estimate $CO_2$ degassing at the catchment scale [e.g., *Abril et al.*, 2014]. Further, our model is unlikely to apply in conditions where $CO_2$ efflux is supply limited, e.g., middle to high pH systems such as glacial-melt [*Thomas and Raiswell*, 1984; *Brown*, 2002] or tufa systems [*Chen et al.*, 2004; *Pedley et al.*, 2009] where speciation of DIC can limit efflux, but flow velocity may still be high. However, to support upscaling, visual classification of water surface state shows promise but requires development and rigorous testing to reduce subjectivity and variation in the estimates.

## References

Abril, G., et al. (2014), Amazon River carbon dioxide outgassing fuelled by wetlands, *Nature*, *505*, 395–398, doi:10.1038/nature12797.

Abril, G., et al. (2015), Technical note: Large overestimation of $pCO_2$ calculated from pH and alkalinity in acidic, organic-rich freshwaters, *Biogeosciences*, *12*, 67–78, doi:10.5194/bg-12-67-2015.

Alin, S. R., M. F. F. L. Rasera, C. I. Salimon, J. E. Richey, G. W. Holtgrieve, A. V. Krusche, and A. Snidvongs (2011), Physical controls on carbon dioxide transfer velocity and flux in low-gradient river systems and implications for regional carbon budgets, *J. Geophys. Res.*, *116*, G01009, doi:10.1029/2010JG001398.

Allen, P. A. (1997), *Earth Surface Processes*, Blackwell Science Ltd., London, U. K.

Aufdenkampe, A. K., E. Mayorga, P. A. Raymond, J. M. Melack, S. C. Doney, S. R. Alin, R. E. Aalto, and K. Yoo (2011), Riverine coupling of biogeochemical cycles between land, oceans, and atmosphere, *Front. Ecol. Environ.*, *9*(1), 53–60, doi:10.1890/100014.

Billett, M. F., and T. R. Moore (2008), Supersaturation and evasion of $CO_2$ and $CH_4$ in surface waters at Mer Bleue peatland, Canada, *Hydrol. Processes*, *22*(12), 2044–2054, doi:10.1002/hyp.6805.

Billett, M. F., M. H. Garnett, and S. M. L. Hardie (2006), A direct method to measure $(CO_2)$-$^{14}$C lost by evasion from surface waters, *Radiocarbon*, *48*, 61–68.

Bock, E. J., T. Hara, N. M. Frew, and W. R. McGillis (1999), Relationship between air-sea gas transfer and short wind waves, *J. Geophys. Res.*, *104*, 25,821–25,831, doi:10.1029/1999JC900200.

Brown, G. H. (2002), Glacier meltwater hydrochemistry, *Appl. Geochem.*, *17*(7), 855–883, doi:10.1016/S0883-2927(01)00123-8.

Butman, D., and P. A. Raymond (2011), Significant efflux of carbon dioxide from streams and rivers in the US, *Nat. Geosci.*, *4*, 839–842, doi:10.1038/NGEO1294.

Charlton, M. B., and N. W. Arnell (2014), Assessing the impacts of climate change on river flows in England using the UKCP09 climate change projections, *J. Hydrol.*, *519*, 1723–1738, doi:10.1016/j.jhydrol.2014.09.008.

Chen, J., D. D. Zhang, S. Wang, T. Xiao, and R. Huang (2004), Factors controlling tufa deposition in natural waters at waterfall sites, *Sediment. Geol.*, *166*, 353–366, doi:10.1016/j.sedgeo.2004.02.003.

Cole, J. J., et al. (2007), Plumbing the global carbon cycle: Integrating inland waters into the terrestrial carbon budget, *Ecosystems*, *10*, 171–184, doi:10.1007/s10021-006-9013-8.

Cox, C., and W. Munk (1954), Measurement of the roughness of the sea surface from photographs of the Sun's glitter, *J. Opt. Soc. Am.*, *44*(11), 838–850, doi:10.1364/JOSA.44.000838.

Dawson, J. J. C., C. Soulsby, M. Hrachowitz, M. Speed, and D. Tetzlaff (2009), Seasonality of $epCO_2$ at different scales along an integrated river continuum within the Dee Basin, NE Scotland, *Hydrol. Processes*, *23*, 2929–2942, doi:10.1002/hyp.7402.

Eugster, W., G. Kling, T. Jonas, J. P. McFadden, A. Wüest, S. MacIntyre, and F. S. Chaplin III (2003), $CO_2$ exchange between air and water in an Arctic Alaskan and midlatitude Swiss lake: Importance of convective mixing, *J. Geophys. Res.*, *108*(D12), 4362, doi:10.1029/2002JD002653.

Frankignoulle, M. (1988), Field measurements of air-sea $CO_2$ exchange, *Limnol. Oceanogr.*, *33*, 313–322.

Gloor, M., R. J. W. Brienen, D. Galbraith, T. R. Feldpausch, J. Schoengart, J.-L. Guyot, J. C. Espinoza, J. Lloyd, and O. L. Phillips (2013), Intensification of the Amazon hydrological cycle over the last two decades, *Geophys. Res. Lett.*, *40*, 1729–1733, doi:10.1002/grl.50377.

Gordon, H. R. (2005), Normalized water-leaving radiance: Revisiting the influence of surface roughness, *Appl. Opt.*, *44*(2), 241–248, doi:10.1364/AO.44.000241.

Gordon, N. D., T. A. McMahon, B. L. Finlayson, C. J. Gippel, and R. J. Nathan (2004), *Stream Hydrology: An Introduction for Ecologists*, 2nd ed., John Wiley, Chichester, U. K.

Herczeg, A. L., and H. R. Hesslein (1984), Determination of hydrogen ion concentration in softwater lakes using carbon dioxide equilibria, *Geochim. Cosmochim. Acta*, *48*, 837–845, doi:10.1016/0016-7037(84)90105-4.

Hofmann, H., A. Lorke, and F. Peeters (2008), The relative importance of wind and ship waves in the littoral zone of a large lake, *Limnol. Oceanogr.*, *53*(1), 368–380, doi:10.4319/lo.2008.53.1.0368.

Hoffmann, M., and H. J. Schellnhuber (2010), Ocean acidification: A millennial challenge, *Energy Environ. Sci.*, *3*, 1883–1896, doi:10.1039/C000820F.

Hope, D., S. M. Palmer, M. F. Billet, and J. J. C. Dawson (2001), Carbon dioxide and methane evasion from a temperate peatland stream, *Limnol. Oceanogr.*, *46*, 847–857, doi:10.4319/lo.2001.46.4.0847.

Hunt, C. W., J. E. Salisbury, and D. Vandemark (2011), Contribution of non-carbonate anions to total alkalinity and overestimation of $p$CO$_2$ in New England and Brunswick rivers, *Biogeosciences*, *8*, 3069–3076, doi:10.5194/bg-8-3069-2011.

Jonsson, A., J. Åberg, A. Lindroth, and M. Jansson (2008), Gas transfer rate and CO$_2$ flux between an unproductive lake and the atmosphere in northern Sweden, *J. Geophys. Res.*, *113*, G04006, doi:10.1029/2008JG000688.

Lauerwald, R., J. Hartmann, N. Moosdorf, S. Kempe, and P. A. Raymond (2013), What controls the spatial patterns of the riverine carbonate system?—A case study for North America, *Chem. Geol.*, *337–338*, 114–127, doi:10.1016/j.chemgeo.2012.11.011.

Liss, P. S., and L. Merlivat (1986), Air-sea gas exchange rates: Introduction and synthesis, in *The Role of Air-Sea Exchange in Geochemical Cycling*, edited by P. Buat-Menard, pp. 113–127, Springer, Netherlands.

Maberly, S. C., P. A. Barker, A. W. Stott, and M. M. De Ville (2013), Catchment productivity controls CO$_2$ emissions from lakes, *Nat. Clim. Change*, *3*, 391–394, doi:10.1038/nclimate1748.

Melack, J. M. (2011), Riverine carbon dioxide releases, *Nat. Geosci.*, *4*, 821–822, doi:10.1038/ngeo1333.

Moog, D. B., and G. H. Jirka (1998), Analysis of reaeration equations using mean multiplicative error, *J. Environ. Eng.*, *124*, 104–110, doi:10.1061/(ASCE)0733-9372(1998)124:2(104).

Moog, D. B., and G. H. Jirka (1999), Air-water gas transfer in uniform channel flow, *J. Hydraul. Eng.*, *125*, 3–10, doi:10.1061/(ASCE)0733-9429(1999)125:1(3).

Neu, V., C. Neill, and A. V. Krusche (2011), Gaseous and fluvial carbon export from an Amazon forest watershed, *Biogeochemistry*, *105*, 133–147, doi:10.1007/s10533-011-9581-3.

Palumbo, J. E., and L. C. Brown (2013), Assessing the performance of reaeration prediction equations, *J. Environ. Eng.*, *140*, doi:10.1061/(ASCE)EE.1943-7870.0000799.

Pedley, H. M., M. Rogerson, and R. Middleton (2009), Freshwater calcite precipitates from in vitro mesocosm flume experiments: A case for biomediation of tufas, *Sedimentology*, *56*, 511–527, doi:10.1111/j.1365-3091.2008.00983.x.

Peter, H., G. A. Singer, C. Preiler, P. Chifflard, G. Steniczka, and T. J. Battin (2014), Scales and drivers of temporal $p$CO$_2$ dynamics in an Alpine stream, *Biogeosciences*, *119*, 1078–1091, doi:10.1002/2013JG002552.

Pinheiro, J., D. Bates, S. DebRoy, D. Sarkar, and R Core Team (2014), nlme: Linear and nonlinear mixed effects models, R package version 3.1-117. [Available at http://CRAN.R-project.org/package=nlme.]

Pinheiro, J. C., and D. M. Bates (2000), *Mixed-Effects Models in S and S-Plus*, Springer, New York.

Preisendorfer, R. W., and C. D. Mobley (1986), Albedos and glitter patterns of a wind-roughened sea surface, *J. Phys. Oceanogr.*, *16*, 1293–1316, doi:10.1117/12.964215.

R Development Core Team (2008), *R: A Language and Environment for Statistical Computing*, R Foundation for Statistical Computing, Vienna, Austria. [Available at http://www.R-project.org.]

Rasera, M. F. F. L., M. V. R. Ballester, and A. V. Krusche (2008), Estimating the surface area of small rivers in the Southwestern Amazon and their role in CO$_2$ outgassing, *Earth Interact.*, *12*, 1–16, doi:10.1175/2008EI257.1.

Rasera, M. F. F. L., A. V. Krusche, J. E. Richey, M. V. R. Ballester, and R. L. Victória (2013), Spatial and temporal variability of $p$CO$_2$ and CO$_2$ efflux in seven Amazonian Rivers, *Biogeochemistry*, *116*, 241–259, doi:10.1007/s10533-013-9854-0.

Raymond, P. A., C. J. Zappa, D. Butman, T. L. Bott, J. Potter, P. Mulholland, A. E. Laursen, W. H. McDowell, and D. Newbold (2012), Scaling gas transfer velocity and hydraulic geometry in streams and small rivers, *Limnol. Oceanogr. Fluids Environ.*, *2*, 41–53, doi:10.1215/21573689-1597669.

Raymond, P. A., et al. (2013), Global carbon dioxide emissions from inland waters, *Nature*, *503*, 355–359, doi:10.1038/nature12760.

Rebsdorf, A., N. Thyssen, and M. Erlandsen (1991), Regional and temporal variation in pH, alkalinity and carbon dioxide in Danish streams, related to soil type and land use, *Freshwater Biol.*, *25*, 419–435, doi:10.1111/j.1365-2427.1991.tb01386.x.

Richey, J. E., J. M. Melack, A. K. Aufdenkampe, V. M. Ballester, and L. L. Hess (2002), Outgassing from Amazonian rivers and wetlands as a large tropical source of atmospheric CO$_2$, *Nature*, *416*, 617–620.

Stumm, W., and J. J. Morgan (1996), *Aquatic Chemistry: Chemical Equilibria and Rates in Natural Waters*, John Wiley, New York.

Thomas, A. C., and R. R. Raiswell (1984), Solute acquisition in glacial melt waters. II. Argentiere (French Alps): Bulk melt waters with open-system characteristics, *J. Glaciol.*, *30*(104), 44–48.

Tranvik, L. J., et al. (2009), Lakes and reservoirs as regulators of carbon cycling and climate, *Limnol. Oceanogr.*, *54*(6), 2298–2314, doi:10.4319/lo.2009.54.6_part_2.2298.

Vihermaa, L. E., S. Waldron, M. H. Garnett, and J. Newton (2014), Old carbon contributes to aquatic emissions of carbon dioxide in the Amazon, *Biogeosciences*, *11*, 3635–3645, doi:10.5194/bg-11-3635-2014.

Waldron, S., E. M. Scott, L. E. Vihermaa, and J. Newton (2014), Quantifying precision and accuracy of measurements of dissolved inorganic carbon stable isotopic composition using continuous-flow isotope-ratio mass spectrometry, *Rapid Commun. Mass Spectro.*, *28*, 1117–1126, doi:10.1002/rcm.6873.

Wallin, M. B., M. G. Öquist, I. Buffam, M. F. Billett, J. Nisell, and K. H. Bishop (2011), Spatiotemporal variability of the gas transfer coefficient (K$_{CO2}$) in boreal streams: Implications for large scale estimates of CO$_2$ evasion, *Global Biogeochem. Cycles*, *25*, GB3025, doi:10.1029/2010GB003975.

Wanninkhof, R. (1992), Relationship between wind speed and gas exchange over the ocean, *J. Geophys. Res.*, *97*, 7373–7382, doi:10.1029/92JC00188.

Zappa, C. J., W. R. McGillis, P. A. Raymond, J. B. Edson, E. J. Hintsa, H. J. Zemmelink, J. W. H. Dacey, and D. T. Ho (2007), Environmental turbulent mixing controls on air-water gas exchange in marine and aquatic systems, *Geophys. Res. Lett.*, *34*, L10601, doi:10.1029/2006GL028790.